PROTEINS: Structure, Function, and Genetics 10:251–259 (1991)

Structure of Ricin A-Chain at 2.5 Å

Betsy J. Katzin, Edward J. Collins, and Jon D. Robertus
Clayton Foundation Biochemical Institute, Department of Chemistry and Biochemistry, University of Texas, Austin, Texas, 78712

ABSTRACT **Ricin has been refined in a crystallographic sense to 2.5 Å resolution and the model for the A-chain (RTA) is described in detail. Because RTA is the first member of the class of plant toxins to be analyzed, this model probably defines the major structural characteristics of the entire family of these medically important proteins. Explanations are provided to rationalize amino acids that are conserved between RTA and a number of homologous plant and bacterial toxins. Eight invariant residues appear to be involved in creating or stabilizing the active site. In the active site Arg180 and Glu177 are hydrogen bonded to each other and also coordinate a water molecule; each of these groups may be important in the N-glycosidation reaction. Several other polar residues may play lesser roles in the mechanism, including tyrosines 80 and 123 and asparagines 78 and 209. A number of conserved hydrophobic residues are seen to cluster within several patches and probably drive the overall folding of the toxin molecule.**

Key words: Ricin A-chain, x-ray structure, active site, conserved residues

INTRODUCTION

Ricin is a heterodimeric protein isolated from the seeds of the castor plant, *Ricinus communis*. The chemical and physical properties of the protein have been reviewed.[1] The ricin toxin A-chain, RTA, is an N-glycosidase of 267 amino acid residues linked by a disulfide bond to the B chain, RTB. RTB is a lectin of 262 residues, with a binding affinity for galactosides. Ricin is an extraordinarily toxic molecule. It binds eucaryotic cell surfaces via the RTB lectin action and enters the cell during endocytosis. RTA escapes from the endosome by an unknown mechanism; in the cytoplasm it attacks ribosomes, removing a specific adenine base from rRNA and thereby inhibiting protein synthesis.[2]

Amino acid sequence comparisons show that ricin is homologous to other heterodimeric plant toxins, such as abrin.[3] In addition, RTA is related to an entire family of single chain ribosome inhibiting proteins (RIPs) from plants. Well-known members of this group include trichosanthin,[4] recently shown to have specific toxicity toward HIV infected cells,[5] pokeweed antiviral protein (PAP),[6] *Mirabilis* antiviral protein (MAP),[7] SO-6,[8] and the inhibitor from barley (BPSI).[9] All of these proteins function by the same N-glycosidase mechanism.[10] Finally, RTA is homologous to a family of medically important bacterial toxins, such as the A-chain of Shiga toxin from *Shigella disentaria,* and the Shiga-like toxin, SLT, from *Escherichia coli.*[11] Both of these proteins are involved in the pathology of various forms of dysentery. Figure 1 shows the amino acid sequence alignment of ricin with other toxins from dicotyledonous plants.

Ricin is the first representative of this class of toxic molecules for which a molecular model, based on x-ray diffraction, could be built;[12] its structure is likely to represent the basic architecture of the entire group. We have used RTA to construct models of abrin and trichosanthin,[4] showing that the sequence differences between RTA and these related toxins could be accommodated with little perturbation in the chain folding and that energy minimization produces a stereochemically plausible model for them. Because of the scientific and commercial interest in plant and bacterial toxins and their engineered derivatives as antiviral agents[5] and in the design of target specific immunotoxins,[13] we present in this study a rather detailed description of the RTA molecule. It is intended to call attention to key structural features that should allow other researchers to evaluate biochemical and mutagenic experiments on a variety of related proteins. The model upon which this description is based was produced by the refinement procedure reported in the previous work.[14]

Folding of Ricin A-Chain

Figure 2 is a ribbon drawing of RTA, viewed down the crystallographic a axis, with the crystallographic c axis vertical in the page. Helices are labeled with capital letters A–H; β sheet strands are labeled a–h. Figure 3 shows the model turned roughly 60° around the C axis from the view in Fig-

Received July 20, 1990; revision accepted February 4, 1991.
Address reprint requests to Jon D. Robertus, Dept. of Chemistry, College of Natural Sciences, University of Texas, Austin, TX 78712-1167.

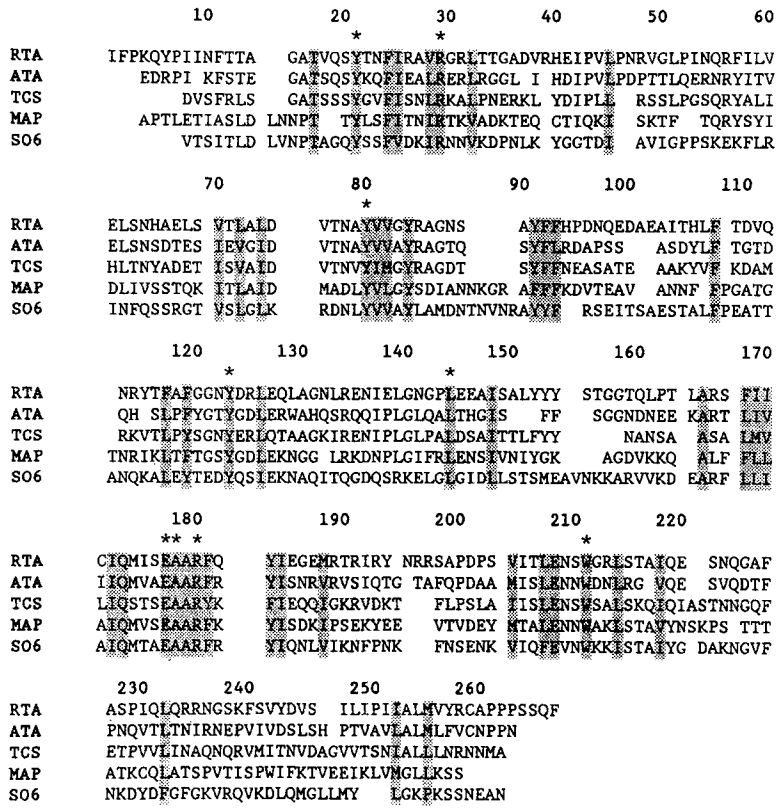

Fig. 1. Sequence comparison of ribosome inhibiting proteins. The amino acid sequences of five proteins from dicotyledonous plants are aligned using the one letter code. RTA is the ricin A-chain,[30,31] ATA is the abrin A-chain,[3] TCS is trichosanthin,[4] MAP is mirabilis antiviral protein,[7] and SO6 is saporin-6.[8] The numbers along the top are RTA sequence numbers. Residues with an * on the top of the column are invariant not only in these proteins but in the barley inhibitor[9] and in the bacterial Shiga-like inhibitor.[11] Residues that are conserved among these proteins are highlighted in the figure. This includes positions that are hydrophobic, although the choice of residue may vary, and for which interactions are described in the text.

ure 2, revealing the toadstoollike shape of the protein. The active site cleft is at the right in this view, and an apparent second cleft is at the left.

In our initial description of ricin, we arbitrarily divided RTA into three folding domains[12,15] based on the local interactions made within each unit and on their compactness. Domain 1 contains residues 1–117, domain 2 is 118–210, and domain 3 is 211–267. A description of the ricin A-chain folding follows, with attention to key features of the secondary structure. Many of the principles of folding and the statistics of residue interactions have been reviewed recently.[16,17]

Figure 2 shows domain 1 to be dominated by a six-stranded β sheet; the strands of this sheet are designated a–f. Two helices, A and B, are also present in the first domain. The detailed hydrogen bonding pattern within the β sheet is given in Figure 4; the helical residues are defined in Table I. The first six residues of RTA interact loosely with the remainder of the protein. The electron density for the first four residues is poorly defined; this suggests disorder in the region, consistent with previous NMR studies.[17]

Strand a of the β sheet lies parallel to strand b; strand f lies parallel to strand e. The remaining strands are arranged in an antiparallel manner. The turn between strands d and e is of the classical type I form; loops of various extent are interposed between the other strands. Modeling studies indicate that when the sequences of several RIPs are compared, insertions and deletions tend to cluster in these loops. One such loop, between strands a and b of the sheet, is formed in part by a helix A. This helix begins at Thr17, the carbonyl O of which is bound to the N of Tyr21; the N of Thr17 is twisted out of helical conformation to donate a bond to the O_G of Ser20. Helix A terminates when the O of Val28 bonds to the N of Arg31 in a turn of 3_{10} helix. Helix B is interposed between strands e and f, running under the plane of the sheet. O_{97} bonds to N_{101} to begin the helix. The helix is capped, in that the side chain O_{D1} of Asn97 bonds forward to N_{100}, which cannot bond carbonyl groups within the helix motif.[16] B also ends in a turn of 3_{10} helix, with O_{104} bonding N_{107}. As discussed below, the loop between strands c and d contains several of the RTA active site residues.

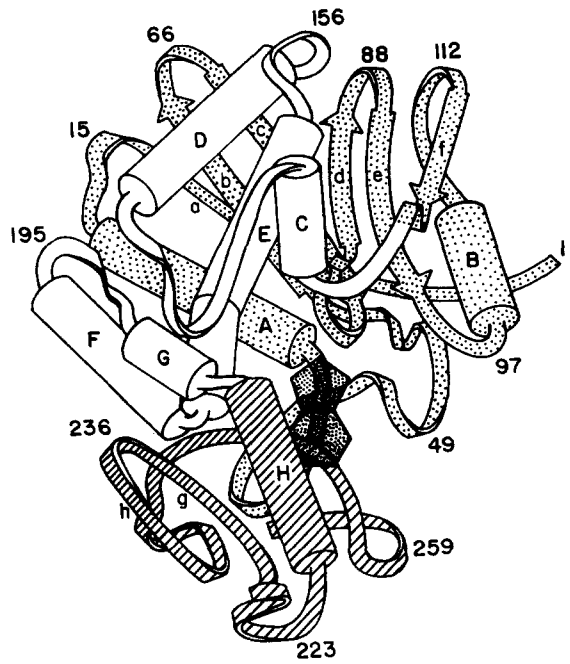

Fig. 2. A ribbon drawing of the ricin A-chain backbone. The helices (cylinders) are labeled A–H along the chain. β sheet (arrows) is labeled a–h. The active site, and binding site for adenine, is indicated by stippled purine symbol. Domain 1, residues 1-117, is dotted, domain 2 (118-210) is open, and domain 3 (211-267) is striped.

The entire six-stranded sheet exhibits a left-handed twist of roughly 110° when viewed along the hydrogen bonds. The βaβ units aAb and eBf both show the righthanded chirality that is commonly seen in this motif.[16]

The second domain is dominated by five helices, labeled C–G. Helix C is about two turns in length and is not capped at either end. D has Pro_{143} at position 3, which is not unusual since this N is not hydrogen bonded as part of the regular helical pattern. Leaving D the chain forms a sharp loop leading to helix E. Part of this loop feeds back to stabilize the C terminal end of D, with the side chain of Ser155 hydrogen bonding to the carbonyl of Tyr152, the formal end of the helix. Helix E is roughly antiparallel to D, although their axes are pitched at 46° with respect to one another. The helices are amphipathic but because they cross at an angle, they interact only locally through hydrophobic forces.

Helix E is the longest one in the protein and in a sense is the core of the molecule. A view of the protein down the E axis shows the helix runs through the molecular center. With its large cylindrical radius, it is the most prominent feature of the protein. As indicated in Figure 2, the helix has a distinct bend of roughly 30° near its C terminal end. This bending allows Glu177 and Arg180 to reach the molecular surface in the active site cavity. The bending requires a local disruption of the helical bonding pattern, which is shown in detail in Figure 5. The normal bonding pattern of the helix is perturbed near the carbonyl of Met174, which is rotated away from the helix axis direction by roughly 50°, allowing it to bond to the hydroxyl group of Tyr21.

Helices E and F form a butt joint, making an angle of 75°. The tightness of the joint or turn is illustrated by the fact that N_{180} donates a weak hydrogen bond to O_{176} as part of the regular pattern of E, whereas O_{182} forms a bond to N_{186} in the regular pattern of F. O_{181} receives bonds from both N_{184} and N_{185} and so participates strongly in the turn but the ϕ and ψ values of −143° and 132° for this conservative Phe181 indicate the residue is not part of either helix. The joint may be partially stabilized by a bond between the side chain of the invariant Arg29 and O_{178} near the C terminal end of E.

Helix F has a distinctly amphipathic nature. Along its solvent face are two ion pairs; Glu185 pairs with Arg189 one turn away and Glu187 pairs with Arg191, again one turn away. On the inside of the helix, Ile184, Met188 and Ile192 anchor three successive turns into the hydrophobic core of the protein. A stretch of seven highly polar residues forms a surface loop leading to helix G. G begins with a Pro (202), a very common phenomenon,[16] and regular bonding continues until N_{210} bonds to O_{206}. Helices F and G are roughly antiparallel, forming an angle of 35°. They interact through hydrophobic contacts in which the side chains of Tyr183 and Ile184 from helix F contact those of Val204 and Leu207 helix G. The polar face of G has an ion pair between Glu187 and Arg191, one turn away. Helices F and G and the loop between them, are rich in Arg residues, creating a positively charged patch on the molecular surface near the back side of the protein.

In our initial description,[12] domain 2 terminates at position 210, which ends helix G, and domain 3 begins at Trp 211, which initiates the regular bonding pattern of helix H. The axis of H is tilted by 55° with respect to that of G, and for this reason it is convenient to consider them not as a single bent helix, but the joining of two distinct helices. The ϕ and ψ angles of Asn210, −110° and 3°, respectively, reflect the perturbation, as does the fact that O_{210} receives strong bonds from both N_{213} and N_{214}. Helix H is capped at its C terminal end with O_{218} bonding to the side chain of Ser221. As indicated in Figure 2, the remaining residues of domain 3 are mostly random coil. Two strands, labeled g and h, resemble an antiparallel tongue, but in fact are rather irregular in structure. Only three hydrogen bonds near the center of the strands exhibit the β-pattern. One striking feature of domain 3 is the very hydrophobic nature of residues near the C terminus; residues 247–257 are Ile-Leu-Ile-Pro-Ile-Ile-Ala-Leu-Met-Val. The mechanism of RTA translocation across membranes is unknown at present, but it is possible

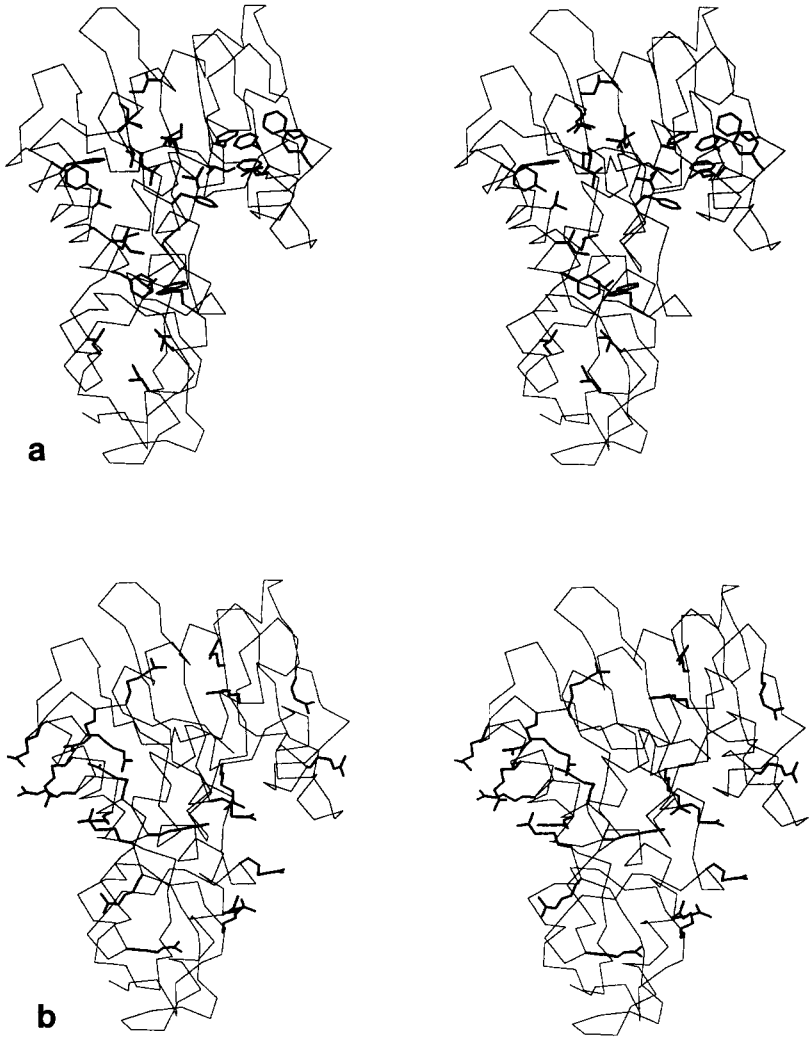

Fig. 3. Side views of ricin A-chain. The a carbon backbone of ricin A-chain is rotated roughly 60° from the view shown in Figure 1, to display the prominent active site cleft, and toadstool shape of the protein. **(a)** The side chains of nonpolar residues conserved in the plant toxins are attached to the Ca backbone. Tyrosines are considered as polar residues for this display, except for Tyr21, a buried residue described in the text. **(b)** Arginine side chains are attached to the Ca backbone; some of these side chains are likely responsible for the binding of RTA to rRNA.

that this tail may insert into membranes to initiate the process.

Contacts Between Domains

To complete a description of RTA, it is important to show how the compact domains, as described above, interact with one another. Because there are so many interactions in a molecule of this size, it is not profitable to make a complete list; the following tries to define the principle contacts of this class of molecules.

The principle forces holding domain 1 to 2 are the hydrophobic interactions along helix E, which is enfolded by the five-stranded mixed sheet of domain 1. Helix E residues Phe168, Ile172, Ile175, and Ala179 on successive turns interact with nonpolar residues

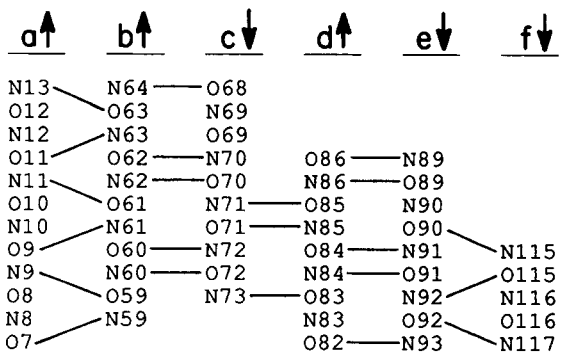

Fig. 4. β sheet hydrogen bond pattern. Ricin A-chain has a prominent six stranded sheet. The bonds between carbonyl oxygens and amido nitrogens are diagrammed.

TABLE I: Helices of Ricin A-Chain

Helix	Residues
A	18–32
B	99–104
C	122–127
D	141–152
E	161–180
F	184–192
G	202–210
H	211–219

from domain I. In particular, the side chain of Phe168 is in hydrophobic interaction with the hydrocarbon side chains of Tyr84, Phe93, Phe117, and Leu126, whereas Ile172 is in contact with side chains of Tyr80, Val81, Tyr123, and Leu126. An inspection of Figure 1 shows that all of these nonpolar residues securing the molecular center are conserved. Ser176 is a polar side chain in this very nonpolar region of the E helix; its buried hydroxyl group makes a strong hydrogen bond (2.75 Å) to O_{79} from the d/e loop of domain 1. It is a constraint of protein folding the most polar atoms within the structure make hydrogen bonds.[17]

Helix D from domain 2 also makes a number of contacts to domain 1, but they are less impressive than those for E. Leu144 and Ile148 make hydrophobic contacts with such domain 1 side groups as Leu62. A number of polar contacts are also made, such as the hydrogen bonding of O_{151} to the Tyr84 hydroxyl.

Helix A of domain 1 lies roughly antiparallel to F of domain 2, with a 21° angle between their axis. The two helices lock like screw threads, yet make relatively few specific interactions. The side chain of F-helix Met188 makes Van der Waals contact with the buried ring of Tyr21.

Domain 1 makes fewer contacts with domain 3 than with domain 2. These contacts all arise because the helix A/strand b loop projects like a finger under domain 2 and reaches the hydrophobic tail of the molecule. Ile42 contacts Ile252 and Met255, whereas Leu45 contacts Leu254 and the edge of the ring from Trp211.

Relatively few contacts are made between domains 2 and 3, and to a good approximation these units are independent. Helix G from domain 2 abuts helix H from domain 3 (at Trp211) as described above. Leu207 from the G helix is in direct contact with leucines 214 and 232 from domain 3. These join additional domain 3 residues, including Phe 240, Val242, Ile247, and Leu248 to form a hydrophobic cluster that presumably governs folding in this region. In addition, these residues form a hydrophobic pocket that holds the C terminal Phe262 of ricin B-chain as discussed in the companion work.[19]

Conserved Residues

Comparison of amino acid sequences between related proteins is a potentially powerful tool in understanding which residues are important for structure or function. Since there is interest in engineering a wide range of plant toxins, it is important to make an effort to understand the roles of the conserved residues in this class.

Figure 1 shows the alignment of amino acid sequences of five RIPs from dicotyledonous plants. Nine residues are invariant not only among these proteins but among all known RIPs, including those of bacterial origin. As developed below, eight of these residues appear to be involved with the structure or action of the catalytic site. There are many conservative but not invariant nonpolar residues that appear to stabilize the toxin folding by their packing interactions.

Figure 6 is a stereo picture of the active site region of RTA. Six of the invariant residues, Tyr80, Tyr123, Glu177, Arg180, and Trp211 are shown, along with three conservative polar residues, Gln173, Glu208, and Asn209. The structure and roles of these residues are discussed below.

Two invariant residues that are not directly in the active site cleft are Tyr21 and Arg29. The side chain of Tyr21 is buried inside the protein, where its hydroxyl group bonds to O_{174} from the E helix. Figure 5 shows that the helix is kinked at this position and that the bend brings active site residues Glu177 and Arg180, residing on this distorted segment of the chain, to the surface of the active site cleft. Presumably Tyr21 is invariant because it is required to stabilize this vital distortion of the E helix. Thus even though it is at the back of the molecule, Tyr21 appears to indirectly contribute to the active site structure.

The invariant Arg29 may also play a role in stabilizing the E helix bend. As shown in Figure 5, its side chain appears to stabilize the distorted end of helix E by hydrogen bonding to O_{178} (and perhaps O_{179}). The bond distances are rather long, however, and it is not clear why other polar residues could not substitute for Arg in this capacity. In RTA, the side chain of Arg29 also forms an ion pair with Glu185, although this is not a highly conserved residue and the pair may be adventitious. Arg29 may also be involved in ribosome recognition at a putative second site discussed below.

As mentioned above, hydrophobic interactions drive protein folding and maintain the structural stability of the protein. There is apparently a selective pressure to preserve the closely interacting side chains, which guarantee a successful atomic packing. This packing can be achieved in a number of similar ways, however, and it is generally understood that substitution of Ile for Leu in a hydrophobic core is generally not significant, whereas substi-

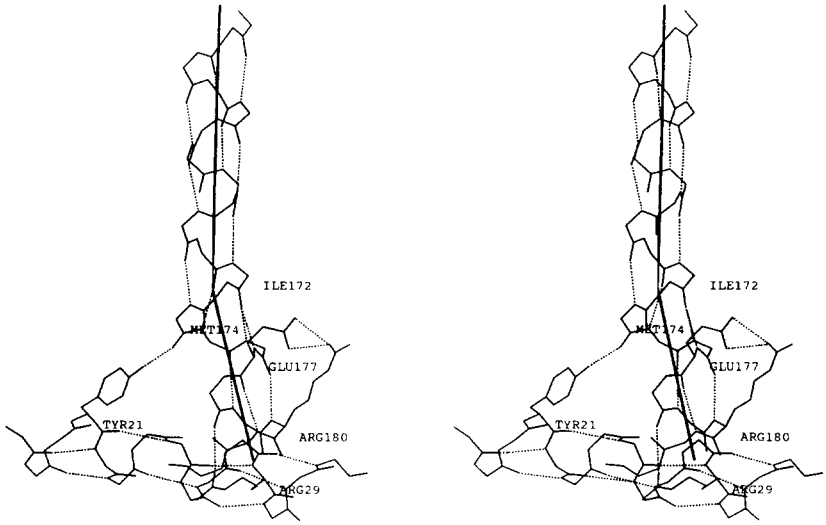

Fig. 5. Distortion of the E helix. The backbone atoms of the A and E helices are shown. The side chains of invariant residues Tyr21 and Arg29 from helix A and Glu177 and Arg180 from E are also shown. The E helix axis is vertical and shows a distinct bend near the bottom. This bend is stabilized by the hydrogen bond from the Tyr21 hydroxyl to the O_{174}.

tution of active site residues involved in catalysis, say Gln for a Glu, can have profound effects. Our observations show that hydrophobic contacts near the active site tend to be more restrictive than those that control domain interactions in more remote areas. Figure 3a shows the positions, in RTA, of residues that are conserved as hydrophobes among the plant toxins. Some packing interactions, such as those of invariant Leu144, are discussed in detail above. Ala178 is the only other invariant aliphatic residue in the toxin class; it is in the active site region pointing away from the solvent. Its C_β contacts the conservative Ile25 and points at the side chain of Tyr21. Any larger residue would interfere with the bond between the invariant Tyr21 and O_{174}, which secures the E helix bend. Phe181 is a very conservative residue, being replaced in only one case by Tyr. It is also in the active site area and with another conserved residue, Leu207, interacts with the invariant Trp211 in the active site cleft. Presumably, their close packing is important to the optimum geometry of the active site. It is also interesting to note the pattern of residues in the main active site peptide. Glu177 and Arg180 are charged and highly polar residues that make their way to the active site surface from the bend of helix E. Ala178 and Phe181 interdigitate with these. By orienting inward toward the hydrophobic core, they presumably are strong determinants of the folding dynamics and the stable state of the active site. In a similar vein, the highly conserved Ile184 contacts both Phe181 and the methylene carbons of the active site Glu177.

It is also noteworthy that several clusters of hydrophobic residues are composed of aromatic groups that tend to pack edgewise in groups of at least three, as described by Burley and Petsko.[20] A prominent example is the cluster of phenylalanines 93, 117, 119, and 168, which are contributed, respectively, from strand e, strand f, the f/C loop, and helix E. Presumably this cluster is conserved because it serves to bind together a number of disparate elements and stabilizes the overall protein architecture. In abrin, probably the most closely related toxin to ricin, these correspond to three leucines and one aromatic residue. As expected, the hydrophobic clustering is retained to stabilize the fold.

The Active Site Structure

Ricin and other plant RIPs are N-glycosidases[2,10] They hydrolytically remove a specific adenine base from a highly conserved loop region of 28S rRNA (A_{4324} in the rat). The RTA Km for reticulocyte ribosomes is 0.1 μM and the kcat is 1,500/min,[21] comparable numbers have been determined by attacking *Artemia* ribosomes with RTA[22] or PAP.[23] The mechanism for this family of N-glycosidases is presently uncertain, but Schramm and coworkers have used kinetic isotope effects to investigate the mechanism of AMP nucleosidase from *Azotobacter vinelandii,* an enzyme that hydrolyzes the adenine base from AMP.[24] Their results are best explained by a transition state with the following characteristics. There is considerable oxycarbonium character in the ribose ring, there is a bonding order between the ribose and the base of about 0.2, water participates as a nucleophile attacking at Cl′ of ribose, and there may be protonation of the leaving group at N_7. This is probably a reasonable working model for the ricin mechanism as well.

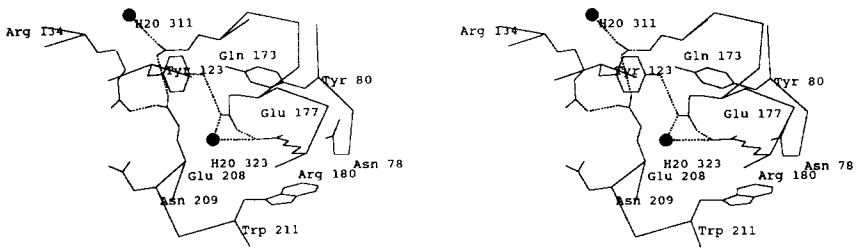

Fig. 6. The active site of ricin A-chain. A stereogram shows invariant and conserved groups in the active site cleft.

We have made a tentative identification of the active site as a prominent cleft in the structure, which contained several invariant amino acids.[15] Free adenine has been diffused into ricin crystals and a 5 Å difference Fourier computed (data not shown). The difference electron density was characterized by a large positive peak in this cleft, supporting the notion that this is indeed the active site. The difference density peak was quite large, being able to accommodate at least two adenines, and too indistinct to position the ring accurately. The general area of product binding is indicated in Figure 2.

Figure 6 shows a close-up view of the active site region. It contains Tyr80, Tyr123, Glu177, Arg180, and Trp211, residues that are invariant in all the toxin sequences known to date, including those from bacteria. The hydroxyl of Tyr 80 makes a strong (2.5 Å) hydrogen bond to O_{121} and helps secure the chain in this area. The other invariant residues participate in a network structure. The side chain of Arg180 lies parallel to the plane of the indole ring of Trp211. The guanidinium protrudes beyond the Trp ring, anchored in place by a strong hydrogen bond between N_{H1} and O_{78}. N_{H2} appears to donate two bonds, one to an active site water molecule (#323) and a second to O_{E2} of Glu177. Glu177 is involved in two additional bonds; O_{E1} hydrogen bonds to water #323 and also to the hydroxyl group of Tyr183. These residues are likely to be involved in either binding the rRNA loop, which is the immediate substrate, or act in catalyzing base excision.

In addition to the invariant residues discussed above, Asn78, Arg134, Gln173, Glu208, and Asn209 are highly conserved active site residues and may play less specific roles in maintaining the active site structure or in the catalytic mechanism. Glu208 forms an ion pair with Arg134 and also hydrogen bonds to the side chain of Glu173. In this position, the methylene carbons of Glu208 contact those of the side chain of Glu177 and appear to form part of one wall of the active site cleft. Gln173 is very conservative and is a polar group inside the protein. Presumably it plays a key role in anchoring Glu208, and it also bonds to a trapped water molecule (#311). Asn209 appears to sit on the molecular surface at the edge of the active site cleft, as does Asn78. They may be involved with RNA base recognition or related functions.

These invariant and conservative residues are the target of site-directed mutagenesis efforts in our laboratory, and several others. A description of some of these mutations and their implications for the mechanism of action are described in a companion work.[22]

Ricin A-chain can excise a single base from eucaryotic ribosomes, from naked 28 S rRNA or from a 35 base synthetic oligonucleotide that contains the conserved stem and loop sequence of the target rRNA.[25] However, the enzyme is about 10,000 times more efficient at attacking whole ribosomes than either naked rRNA or the synthetic substrate. It has been suggested that the toxin may recognize higher order RNA structure and not simply a sequence of bases.[25] The active site cleft appears to be large enough to accommodate a loop of single stranded RNA but probably cannot bind a double helical stem. Ribosome recognition may be accomplished at some other site on the enzyme.

The ribosome substrate is clearly much larger than ricin and so some rather novel interactions may be made in the recognition process. In addition to the specific recognition of the target base sequence, RTA may bind the ribosome by less specific contacts to the rRNA or to ribosomal proteins. These may constitute a first level of recognition that orients the enzyme to make the very specific contacts necessary for hydrolysis of a single base from among thousands. The hypothesis of such an extended binding site seems consistent with the observed Km for ribosomes and the poor attack on even extensive fragments of RNA containing the target sequence. At this time we have no idea which portions of RTA might be involved in this putative extended site. It is interesting to consider, however, that RNA binding might involve arginine residues that can form ion pairs with a polynucleotide backbone. Figure 3b shows the positions of Arg side chains on the enzyme. A number of residues in addition to the invariant Arg180 line the active site cleft. On the back side of the molecule is an apparent second cleft that

also is bordered by Arg residues. One of these, Arg29, is invariant and may be a candidate for some role in RNA binding.

Solvent Structure and Glycosylation

During the refinement of ricin, 120 well-occupied water molecules were identified around the molecular surface of ricin.[14] It is interesting that solvating water molecules are most common around loops, whereas secondary structure, even on the molecular surface, is poorly solvated. The polar atoms of secondary structure are often hydrogen bonded to other protein groups rather than making adventitious bonds to water.

Several water molecules appear to play an integral role in the protein structure. One example is the trapped water 331 whose interactions with Gln 173 are discussed above. The temperature factor for the water is low (about 25 Å^2) and attests to its stability in the structure. In essence it solvates two buried polar atoms, but is virtually cut off from contact with the bulk solvent. There are several other trapped waters within RTA and a number that are held quite firmly by surface loops.

Ricin A-chain is known to have two potential glycosylation sites at Asn10 and Asn236. In some forms, however, only the first site is modified,[26] whereas in other strains there appears to be a heterogeneous modification of both sites.[27] As discussed in the work on crystallographic refinement, the crystals of ricin appear to have selected for those molecules in which the A-chain is unmodified, although both B-chain high mannose moieties are clearly visible in the electron density map.[14] In fact, the crystal packing is such that the Asn10 region of one protein is in contact with a symmetry related molecule near its Asn236 region. Glycosylation at both sites would preclude this packing, and it appears that it would be difficult to accommodate even one carbohydrate chain in this crystal form.

Cloned A-Chain

The structure described above is A-chain from intact heterodimeric ricin. It is carried into cells in association with B-chain and released. The forces holding the chains together are hydrophobic[28] and most of the contacts with B-chain are made by domain 3 of RTA.[19] It is reasonable to assume that chain separation exposes these oily surfaces to the solvent and may trigger some rearranagement of RTA. This putative alteration may serve several functions. It may initiate membrane translocation, perhaps by inserting the nonpolar side chains of the region into the membrane. It may also be that the rearrangement causes a subtle adjustment of active site residues, activating the enzyme, which is inactive as a heterodimer.[1] We have crystallized A-chain expressed from a gene cloned into *Escherichia coli*,[29] and have collected 1.9 Å data on the crystals. Efforts are presently underway to solve the structure by molecular replacement and subsequent crystallographic refinement. Comparison of the two structures may shed light on some of these questions.

ACKNOWLEDGMENTS

We are grateful to Michael Ready for helpful discussions and to Raquelle Smalley for her help in preparing the figures. This work was supported by grants GM 30048 and GM 35989 from the National Institutes of Health and by a grant from the Foundation for Research.

REFERENCES

1. Olnes, S., Pihl, A. The molecular action of toxins and viruses. In: "The Molecular Action of Toxins and Viruses," Cohen, P. and Van Heynigen, S. (eds.). New York: Elsevier, 1982:52–105.
2. Endo, Y., Tsurugi, K. RNA N-glycosidase activity of ricin A-chain. J. Biol. Chem. 262:8128–8130, 1987.
3. Funatsu, G., Taguchi, Y., Kamenosono, M., Yanaka, M. The complete amino acid sequence of the A-chain of abrina, a toxic protein from the seeds of Abrus precatorius. Agric. Biol. Chem. 52:1095–1097, 1988.
4. Collins, E.J., Robertus, J.D., LoPreti, M., Stone, K.L., Williams, K.R., Wu, P., Hwang, K., Piatak, M. Primary amino acid sequence of a-trichosanthin and molecular models for abrin A-chain and α-trichosanthin. J. Biol. Chem. 265:8665–8669, 1990.
5. McGrath, M.S., Hwang, K.M., Caldwell, S.E., Gaston, I., Luk, K.C., Wu, P., Ng, V.L., Crowe, S., Daniels, J., Marsh, J., Deinhart, Y., Lekas, P.V., Vennari, J.C., Yeung, H.W., Lifson, J.D. GLQ223: An inhibitor of human immunodeficiency virus replication in acutely and chronically infected cells of lymphocyte and mononuclear phagocyte lineage Proc. Natl. Acad. Sci. USA 86:2844–2848 1989.
6. Ready, M., Wilson, K. Piatak, M. Robertus, J.D. Ricin-like plant toxins are evolutionarily related to single-chain ribosome-inhibiting proteins from *Phytolacca*. J. Biol. Chem. 259:15252–15256 1984.
7. Habuka, N., Murakami, Y., Noma, M., Kudo, T., Horikoshi, K. Amino acid sequence of *Mirabilis* antiviral protein, total synthesis of its gene and expression in *Escherichia coli*. J. Biol. Chem. 264:6629–6637, 1989.
8. Benatti, L., Saccardo, M.B., Dani, M., Nitti, G., Sassano, M., Lorenzetti, R., Lappi, D.A., Soria, M. Nucleotide sequence of cDNA coding for saporin-6, a type-1 ribosome-inactivating protein from Saponaria officinalis. Eur. J. Biochem. 183:465–470, 1989.
9. Asano, K., Svensson, B., Svendsen, I., Poulsen, P., Roepstorff, P. The complete primary structure of protein synthesis inhibitor II from barley seeds. Carlsberg Res. Commun. 51:129–141, 1986.
10. Endo, Y., Tsurgi, K., Lambert, J.M. The site of action of six different ribosome-inactivating proteins from plants on eukaryotic ribosomes: the RNA N-glycosidase activity of the proteins. Biochem. Biophys. Res. Comm. 150:1032–1036, 1988.
11. Calderwood, S.B., Auclair, F., Donohue-Rolfe, A., Keusch, G.T., Mekalanos, J.J. The nucleotide sequence of the shiga-like toxin genes of *Escherichia coli*. Proc. Natl. Acad. Sci. USA 84:4364–4368, 1987.
12. Montfort, W., Villafranca, J.E., Monzingo, A.F., Ernst, S., Katzin, B., Rutenber, E., Xuong, N.H., Hamlin, R., Robertus, J.D. The three-dimensional structure of ricin at 2.8 Å. J. Biol. Chem. 262:5398–5403, 1987.
13. References in: "Immunotoxins," Frankel, A.E. (ed.) Boston: Kluwer Academic, 1988.
14. Rutenber, E., Katzin, B.J., Collins, E.J., Mlsna, D., Ernst, S.E., Ready, M.P., Robertus, J.D. The cyrstallographic refinement of ricin at 2.5 Å resolution. Proteins 10:240–250, 1991.
15. Ready, M.P., Katzin, B.J., Robertus, J.D. Ribosome-inhibiting proteins, retroviral reverse transcriptases, and

RNase H share common structural elements. Proteins 3: 53–59, 1988.
16. Richardson, J.S., Richardson, D.C. Principles and patterns of protein conformation. In: "Prediction of Protein Structure and the Principles of Protein Conformation," Fasman, G.D. (ed.). New York:Plenum Press, 1989:1–98.
17. Alber, T. Stabilization energies of protein conformation. In: "Prediction of Protein Structure and the Principles of Protein Conformation," Fasman, G.D. (ed.). New York:Plenum Press, 1989:161–192.
18. Bushuev, V., Tonevitsky, A. High mobility of N-terminal parts of A and B subunits of ricin. J. Biomol. Struct. and Dynamics 6:1061–1070, 1989.
19. Rutenber, E., Robertus, J.D. The structure of ricin B chain at 2.5 Å resolution, and its interaction with A chain. Proteins 10:260–269, 1991.
20. Burley, S.K., Petsko, G.A. Aromatic-aromatic interaction: A mechanism of protein structure stabilization. Science 229:23–28, 1985.
21. Olsnes, S., Fernandez-Puentes, C., Carrasco, L., Vasquez, D. Ribosome inactivation by the toxic lectins abrin and ricin: kinetics of the enzymic activity of the toxin A-chains. Eur. J. Biochem. 60:281–288, 1975.
22. Ready, M.P., Kim, Y., Robertus, J.D. Site directed mutagenesis of ricin A chain and implications for the mechanism of action. Proteins 10:270–278, 1991.
23. Ready, M., Bird, S., Rothe, G., Robertus, J.D. Requirements for antiribosomal activity of pokeweed antiviral protein. Biochem. Biophys. Acta 740:19–28, 1983.
24. Mentch, F., Parkin, D.W., Schramm, V.L. Transition-state structures for N-glycoside hydrolysis of AMP by acid and by AMP nucleosidase in the presence and absence of allosteric activator. Biochemistry 26:921–930, 1987.
25. Endo, Y., Chan, Y.L., Lin, A., Tsurugi, K., Wool, I.G. The cytotoxins a-sarcin and ricin retain their specificity when tested on a synthetic oligoribonucleotide (35-mer) that mimics a region of the 28 S ribosomal ribonucleic acid. J. Biol. Chem. 263:7917–7920, 1988.
26. Kimura, Y., Hase, S., Kobayashi, Y., Kyogoku, Yd., Ikenaka, T., Funatsu, G. Structures of sugar chains of ricin D. J. Biochem. 103:944–949, 1988.
27. Foxwell, B.M.J., Donovan, T.A., Thorpe, P.E., Wilson, G. The removal of carbohydrates from ricin with endoglycosidases H, F, and D and a-mannosidase. Biocim. Biophys. Acta 840:193–203, 1985.
28. Lewis, M.S., Youle, R.J. Ricin subunit association: Thermodynamics and the role of the disulfide bond in toxicity. J. Biol. Chem. 261:11571–11577, 1986.
29. Robertus, J.D., Piatak, M., Ferris, R., Houston, L.L. Crystallization of ricin A chain obtained from a cloned gene expressed in *Escherichia coli*. J. Biol. Chem. 262:19–20, 1987.
30. Lamb, F.I., Roberts, L.M., Lord, J.M. Nucleotide sequence of cloned cRNA coding for preproricin. Eur. J. Biochem. 148:265–270, 1985.
31. Halling, K.C., Halling, A.C., Murray, E.E., Ladin, B.F., Houston, L.L., Weaver, R.F. Genomic cloning and characterization of a ricin gene from *Ricinus communis*. Nucl. Acids Res. 13:8019–8033, 1985.